

# Fast Grating-based X-ray Phase-contrast Tomosynthesis

Yan Xi and Jun Zhao\*, *Member, IEEE*

**Abstract**—As an imaging technique with low radiation dose and improved contrast, digital x-ray tomosynthesis is widely used in clinical diagnoses. Based on the superior capability of x-ray phase-contrast imaging (PCI) techniques for imaging low density materials, the combination of X-ray tomosynthesis and PCI can potentially provide higher efficiency in the detection of soft tissues. The goal of this work was to develop a fast imaging method for phase-contrast tomosynthesis, called fast grating-based phase-contrast tomosynthesis (GPC-Tomo), which integrates tomosynthesis with a grating-based PCI technique. Following the interlaced phase-stepping (PS) data collection method, which is much faster than conventional PS method, we propose a novel image reconstruction method called inner-focusing (IF) reconstruction for the fast GPC-Tomo. The proposed IF reconstruction method was validated by real experiments and the results suggested its effectiveness in achieving a fast GPC-Tomo.

## I. INTRODUCTION

Digital X-ray tomosynthesis is a technique for producing cross-sectional images from a limited range of viewing angles. It is widely used in diagnostic imaging applications as it requires a low radiation dose and provides improved image contrast [1]. The mechanism of conventional x-ray imaging is based on the absorption property of materials, which is limited when imaging low density materials. Compared with conventional absorption-based x-ray imaging, x-ray phase-contrast imaging (PCI) techniques have gained special attention in recent years for their superior soft tissue imaging capability [2-4]. Among the various proposed methods for PCI, the grating-based technique has been extensively developed and has been successfully extended to use with a laboratory x-ray tube [5-7]. With future translation into the clinic, it shows promise in many imaging applications [8].

The PCI technique has superior soft-tissue imaging capability while x-ray tomosynthesis has improved image contrast. Combining the two techniques can therefore greatly improve the performance of x-ray imaging in clinical use [9]. The grating-based phase-contrast tomosynthesis (GPC-Tomo) method has been described in previous studies [10, 11]. Preliminary investigations demonstrated that it had excellent performance in imaging low density materials and provided more contrast mechanisms, absorption contrast, phase contrast and scattering contrast. However, these implementations have simply replaced the per projection angle image acquisition procedure of conventional x-ray tomosynthesis with a phase-stepping (PS) scan, which is the standard data

acquisition scheme in grating-based PCI. The straightforward packing of GPC-Tomo results in a high radiation dose and long data acquisition process.

In the present paper, we propose a fast imaging method for GPC-Tomo. Following the interlaced PS method where the sample rotation and the grating stepping occur simultaneously [12, 13], a novel image reconstruction method was developed for the proposed fast GPC-Tomo, which we call the inner-focusing (IF) reconstruction method.

## II. MATERIALS AND METHODS

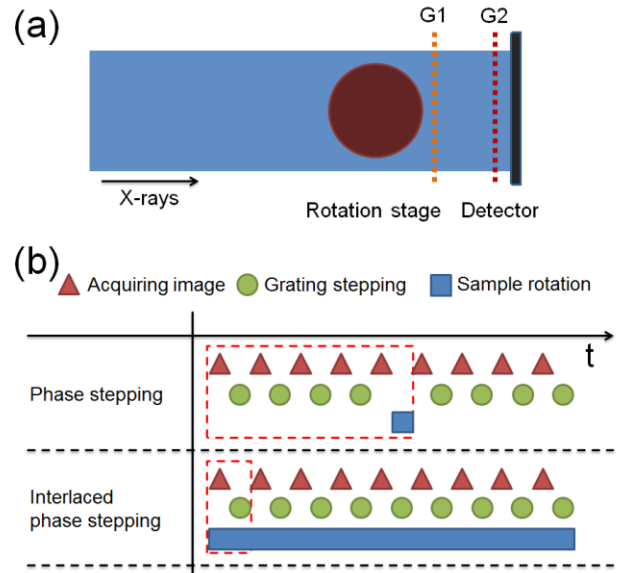


Figure 1. (a) Schematic representation of GPC-Tomo with synchrotron x-rays. The data collection schemes with PS, and interlaced PS methods are illustrated in (b). The red dashed boxes indicate the data collection procedure at each projection angle.

The GPC-Tomo system is similar to a commercial x-ray tomosynthesis system except that a grating interferometer, including G0, G1 and G2, is integrated into its rotation gantry. In this paper, a proof-of-principle experimental demonstration of GPC-Tomo is carried out using the third generation synchrotron radiation. The following description is mainly focused on the parallel-beam case. Fig. 1(a) shows the synchrotron radiation-based GPC-Tomo system, where partial coherent x-rays illuminate the sample and are then analyzed using gratings G1 and G2. In the x-ray tube case, a source grating G0 is employed to create an array of individually coherent x-rays. The three-grating system is a promising way to implement a tomosynthesis scan for clinical imaging applications as it lowers the requirements of partial coherence of the incident x-rays.

Two kinds of data collection schemes for performing GPC-Tomo are plotted in Fig. 1(b). Method 1 shows the

\*Asterisk indicates corresponding author.

Research supported by National Basic Research Program of China (973 Program; 2010CB834302).

Yan Xi is with the School of Biomedical Engineering, Shanghai Jiao Tong University, Shanghai, China 200030 (e-mail: yanxi@sjtu.edu.cn).

Jun Zhao is with the School of Biomedical Engineering, Shanghai Jiao Tong University, Shanghai, China 200030 (e-mail: junzhao@sjtu.edu.cn).

standard data acquisitions of conventional GPC-Tomo in which several projections are captured per projection angle to extract differential phase-contrast images. The stop-and-go motion of the PS approach in conventional GPC-Tomo is time consuming. Employing the interlaced PS method for data collection, the sample rotation and grating stepping occur at the same time, which means that it is a continuous-movement mode and only one image is recorded per projection angle, as illustrated by Method 2 in Fig. 1(b). As the data acquisition is implemented in a continuous rotation mode, the scanning of the interlaced-PS-based GPC-Tomo can be completed within a much shorter time than the conventional one, called fast GPC-Tomo.

In the conventional GPC-Tomo system, the PS approach is adopted to retrieve the differential phase-contrast images about the sample at each projection angle. According to the data acquisition scheme of Method 1, at each projection angle, the grating G1 moves perpendicularly to the grating lines until covering a period of grating G2. The measured intensity at each pixel (indexed by  $t$ ) oscillates as a function of the relative displacement  $x$ , expressed as:

$$P_x(t) = \sum_i a_i(t) \cos\left(\frac{2\pi}{g_2}x + \varphi_i\right) \approx a_0(t) + a_1(t) \cos\left(\frac{2\pi}{g_2}x + \varphi_1\right) \quad (1)$$

where  $g_2$  denotes the period of grating G2,  $a_0$  represents the transmittance of the sample and gratings, and  $\varphi_1$  is the phase shift signal of the incident X-rays. The analysis of the intensity oscillations at each pixel with/without the sample can yield information about the transmittance  $a_0$ , differential phase contrast signal  $\varphi$  and scattering property  $\frac{a_1}{a_0}$  of the sample.

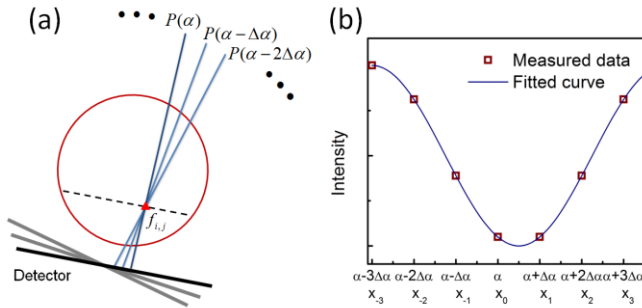


Figure 2. (a) Imaging geometry of the fast GPC-Tomo. (b) plots the measured x-ray intensities that are from neighboring viewings and go through pixel  $f_{i,j}$ .  $\alpha + i\Delta\alpha$  and  $x_i$  are variables of the oscillation curve. They are corresponding to each other as the sample rotation and grating stepping occur simultaneously.

The imaging geometry of the fast GPC-Tomo system is shown in Fig. 2(a) where the projection angle is given by  $\alpha$ , and the scanned object  $f$  is projected onto the detector plane represented by  $P(\alpha)$ . In the fast GPC-Tomo system, the transverse movement of G1 occurs along with the sample rotation. Thus, the intensity oscillation at each pixel is a function of both the relative displacement of grating G1 and the variation of the projection angle. The intensities of the oscillation curve are plotted in Fig. 2(b) in which  $\Delta\alpha$  is the angle interval of captured projection images. As the sample rotation and grating stepping occur at the same time, the

projection angle  $\alpha + i\Delta\alpha$  and the grating displacement  $x_i$  correspond to each other. Thus, it is an ill-posed problem to retrieve the differential phase-contrast signals with the analysis method used in conventional GPC-Tomo. In the reconstruction stage of the fast GPC-Tomo, X-rays from neighboring viewing angles are used to compose a stepping cycle. Differing from the conventional interlaced PS method, when the IF reconstruction method is adopted, x-rays that go through the reconstructed pixel are selected to retrieve the differential phase-contrast signal. This is the so-called inner focusing process. The imaging geometry of the IF method is shown in Fig. 2(a), where  $f_{i,j}$  is the reconstructed point in the target plane indicated by the dashed line. As the grating G1 steps along the rotation of the sample, their intensity values oscillate in a rough approximation to a cosine function, as plotted in Fig. 2(b).

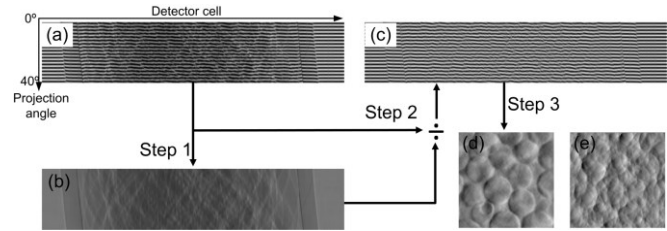


Figure 3. Workflow of the image reconstruction process. (a) is the sinogram of the scanned object over 40 degrees, collected with the fast GPC-Tomo technique. The corresponding absorption map (b) is calculated according to (2). (c) is the normalized sinogram. The reconstruction result is shown in (d). (e) is a differential phase-contrast projection image of the object.

Compared with the data acquisition scheme of conventional GPC-Tomo, the data collected by the fast GPC-Tomo system is incomplete. Each measurement in a stepping cycle fluctuates by the transmittance  $a_0$  with different viewing angle  $\alpha$ . Thus, the first step of the IF reconstruction method is to remove the influence of the transmittance of the sample. The measured X-rays are normalized by the averaged intensities over a period of grating scanning which includes  $N$  steps. The mean transmitted intensity,  $a'_0(\alpha, t)$ , is calculated over a rotational angular arrangement which is equal to one stepping period of grating G1, expressed as

$$a'_0(\alpha, t) = \frac{1}{N} \sum_{i=0}^{N-1} P(\alpha', t') \quad (2)$$

where  $\alpha' = \alpha - \left(\frac{n}{2}\right) \Delta\alpha$  and  $t' = x \cos(\alpha') + y \sin(\alpha')$ . The process of sample rotation or grating stepping is indexed by  $i$  where  $i = 0, 1, 2, \dots, N-1$ . The projection position of  $f_{i,j}$  located on the detector plane is given by  $t'$ , making X-rays pass through the reconstruction point. The raw data collected by the interlaced PS method is shown in Fig. 3(a). The sinogram of the averaged transmittance map of the object is given in Fig. 3(b). Subsequently, the mean transmitted intensities are utilized to normalize the corresponding projection data acquired by the fast GPC-Tomo approach, expressed as

$$P'(\alpha, t) = \frac{P(\alpha, t)}{a'_0(\alpha, t)} \approx 1 + s \cdot \cos\left(\frac{2\pi}{g_2}x + \varphi_1\right) \quad (3)$$

where  $s$  denotes the scattering information of the scanned object. The normalized projection image  $P'$  (Fig. 3(c)) is quite close to the ideal condition that the phase-contrast signal  $\varphi_1$  is

the only variable. As the pixel  $f_{i,j}$  in the scanned object is located at different positions in the horizontal detector array with different projection angles, we track its projection along a particular trajectory in the normalized sinogram (Fig. 3(c)) making incident x-rays focus at the reconstruction point  $f_{i,j}$ . As suggested by (3), it can be seen that the tracked signal oscillates with a cosine function. Thus, the phase-contrast signal can be determined by fitting a cosine function according to Eq. 3 using the Levenberg-Marquardt algorithm [14] and then mapping it to the reconstructed longitudinal image. If the angle divergence is considered in the reconstruction, an angular weighting  $w$  can be calculated according to the angle deflection, and integrated into the nonlinear fitting procedure. The workflow of the IF reconstruction algorithm for the fast GPC-Tomo is shown in Fig. 3. One of the differential phase-contrast slices reconstructed with the fast GPC-Tomo is shown in Fig. 3(d). Fig. 3(e) shows an X-ray phase-contrast projection image of the phantom. In the current implementation, we adopt the classic shift-and-add method to reconstruct slice images [15]. Advanced reconstruction methods for tomosynthesis can also be integrated into the workflow [16]. Limited by our real experiments, the algorithm is described with a parallel X-ray beam condition. The proposed fast GPC-Tomo and IF reconstruction algorithm are also suitable for the X-ray fan-beam case.

### III. RESULTS

In our biological imaging experiment, a paw excised from a C57/Black6 mouse (weight 24 g) was utilized to investigate the performance of the proposed fast GPC-Tomo, as shown in Fig. 4(a). The sample was scanned by a grating-based interferometer installed into the BL13W beam line at Shanghai Synchrotron Radiation Facility (SSRF). X-ray tomography of the phantom was carried out at 20 keV, in which 720 projection images were recorded over 180 degrees. The phase shift of grating G1 was designed to be  $\pi/2$ , and its period is 2.396  $\mu\text{m}$ . The period of grating G2 is 2.4  $\mu\text{m}$ . The inner distance between G1 and G2 was 46.4 mm. In each phase-stepping scan, the grating G1 moved along the transverse direction perpendicular to the grating line direction with 12 steps to cover one full period of the grating G2. Projection images were recorded by a CCD detector (Photonic Science, East Sussex, UK) having an effective pixel size of 9  $\mu\text{m}$ ; the exposure time for each image was 12 ms. To simulate the data collection scheme of the conventional GPC-Tomo and the proposed fast GPC-Tomo as illustrated in Fig. 1(b), the complete CT data set was rearranged into specific tomosynthesis data sets according to their respective data collection protocols.

Fig. 4(b) shows the resulting differential phase-contrast projection image of the mouse paw. It can be seen that details of the specimen overlapped. In our experiment, the specimen was scanned with the data collection scheme of fast GPC-Tomo over  $40^\circ$  with  $\Delta\alpha = 0.25^\circ$ . Twelve steps of grating G1 movements cover one period of grating G2. Two of its longitudinal slices are reconstructed according to the inner-focusing reconstruction method (Fig. 4(c-d)). In Fig. 4(c-d), as expected, the bone structures are clearly visible. However, low density materials such as the fine hairs on the paw can also be observed, as indicated by red arrows in Fig. 4(c-d).

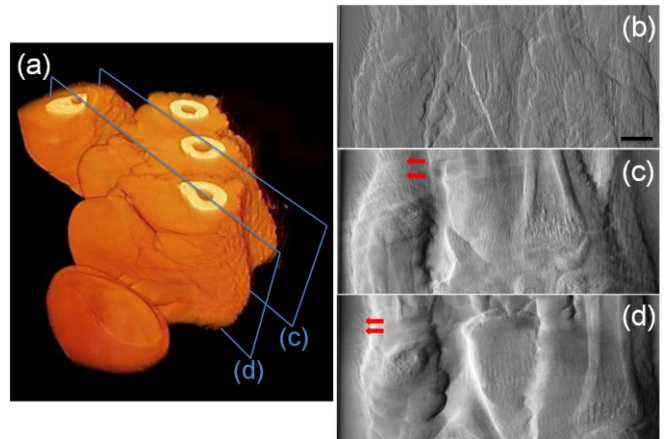


Figure 4. (a) Three-dimensional visualization of a mouse paw. (b) shows the differential phase-contrast projection image of the mouse paw. Bar: 1 mm. (c) and (d) are the reconstructed slice images of the specimen with the fast GPC-Tomo. The target slices are marked by blue boxes in (a). Red arrows in (c-d) indicate reconstructed fine hairs on the paw.

### IV. DISCUSSION AND CONCLUSION

Combining the advantages of the X-ray tomosynthesis technique and X-ray PCI technique, the GPC-Tomo technique can potentially improve the soft-tissue discrimination capability of X-ray imaging. Differing from the conventional, straightforward-packing GPC-Tomo system, the proposed fast GPC-Tomo can be implemented in scans with a continuous rotation method that is common in commercial X-ray imaging systems. Without the stop-and-go motion used in the conventional GPC-Tomo technique, the data acquisition scheme of the fast GPC-Tomo can significantly reduce scanning time. This is achieved in conjunction with a special data collection protocol and corresponding reconstruction algorithm to enable fast GPC-Tomo. As the interlaced PS method has been demonstrated that it can reduce the radiation dose that is necessary while keeping the same acceptable image quality [13]. In our experiments, GPC-Tomo was simulated with a synchrotron light source. It can also be implemented with a laboratory x-ray tube by installing another grating G0 as reported by previous studies [5]. The proposed IF reconstruction method verified by current parallel-beam X-ray studies can also be easily extended to the fan-beam case. Thus, there is potential to further translate the proposed GPC-Tomo into clinical applications. Benefitting from the excellent ability of the PCI technique to discern soft tissues with the improved image contrast of tomosynthesis technique, the fast GPC-Tomo may have broad potential in clinical diagnostic imaging applications.

In conclusion, a fast imaging method for GPC-Tomo has been proposed. GPC-Tomo is based on the PCI technique, which is capable of imaging low density materials. Thus, a technique combining PCI with tomosynthesis can provide enhanced soft tissue discrimination compared with conventional absorption-based tomosynthesis techniques. By adopting the interlaced PS data collection scheme and the proposed IF reconstruction method, the long imaging time required by conventional GPC-Tomo can be effectively reduced. The proposed fast GPC-Tomo method represents an implementation of an X-ray imaging system with superior performance to low density materials and improved image

contrast with low radiation dose. This work proves the feasibility of performing grating-based phase-contrast X-ray tomosynthesis to provide improved imaging capability.

#### ACKNOWLEDGMENT

This work was performed at the BL13W beam line of Shanghai Synchrotron Radiation Facility (SSRF)

#### REFERENCES

- [1] D. J. Godfrey, "Digital x-ray tomosynthesis: current state of the art and clinical potential," *Physics in medicine and biology*, vol. 48, p. R65, 2003.
- [2] D. Gao, A. Pogany, A. W. Stevenson, and S. W. Wilkins, "Phase-contrast radiography," *Radiographics*, vol. 18, pp. 1257-1267, 1998.
- [3] T. Weitkamp, A. Diaz, C. David, F. Pfeiffer, M. Stampanoni, P. Cloetens, and E. Ziegler, "X-ray phase imaging with a grating interferometer," *Opt. Express*, vol. 13, pp. 6296-6304, 2005.
- [4] D. Chapman, W. Thomlinson, R. Johnston, D. Washburn, E. Pisano, N. Gmür, Z. Zhong, R. Menk, F. Arfelli, and D. Sayers, "Diffraction enhanced x-ray imaging," *Physics in medicine and biology*, vol. 42, p. 2015, 1997.
- [5] F. Pfeiffer, T. Weitkamp, O. Bunk, and C. David, "Phase retrieval and differential phase-contrast imaging with low-brilliance X-ray sources," *Nature Physics*, vol. 2, pp. 258-261, 2006.
- [6] M. Stampanoni, Z. Wang, T. Thüring, C. David, E. Roessl, M. Trippel, R. A. Kubik-Huch, G. Singer, M. K. Hohl, and N. Hauser, "The First Analysis and Clinical Evaluation of Native Breast Tissue Using Differential Phase-Contrast Mammography," *Investigative Radiology*, 2011.
- [7] A. Tapfer, M. Bech, B. Pauwels, X. Liu, P. Bruyndonckx, A. Sasov, J. Kennntner, J. Mohr, M. Walter, and J. Schulz, "Development of a prototype gantry system for preclinical x-ray phase-contrast computed tomography," *Medical physics*, vol. 38, 2011.
- [8] R. Lewis, "Medical phase contrast x-ray imaging: current status and future prospects," *Physics in medicine and biology*, vol. 49, p. 3573, 2004.
- [9] J. C. Hammonds, R. R. Price, E. F. Donnelly, and D. R. Pickens, "Phase-contrast digital tomosynthesis," *Medical physics*, vol. 38, p. 2353, 2011.
- [10] Z. Wang, Z. Huang, Y. Xiao, L. Zhang, and K. Kang, "Multiple information tomosynthesis with grating-based phase-contrast imaging," 2009, p. 72581N.
- [11] W. Zhentian, K. Kejun, H. Zhifeng, Z. Li, C. Zhiqiang, D. Fei, and F. Qiaoguang, "Differential phase-contrast tomosynthetic experimental system with weakly coherent hard X-rays," in *Nuclear Science Symposium Conference Record, 2008. NSS '08. IEEE, 2008*, pp. 3889-3891.
- [12] I. Zanette, M. Bech, F. Pfeiffer, and T. Weitkamp, "Interlaced phase stepping in phase-contrast x-ray tomography," *Applied Physics Letters*, vol. 98, p. 094101, 2011.
- [13] I. Zanette, M. Bech, A. Rack, G. Le Duc, P. Tafforeau, C. David, J. Mohr, F. Pfeiffer, and T. Weitkamp, "Trimodal low-dose X-ray tomography," *Proceedings of the National Academy of Sciences*, vol. 109, pp. 10199-10204, 2012.
- [14] G. A. F. Seber and C. J. Wild, *Nonlinear regression* vol. 503: LibreDigital, 2003.
- [15] D. G. Grant, "Tomosynthesis: A three-dimensional radiographic imaging technique," *Biomedical Engineering, IEEE Transactions on*, pp. 20-28, 1972.
- [16] T. Wu, R. H. Moore, E. A. Rafferty, and D. B. Kopans, "A comparison of reconstruction algorithms for breast tomosynthesis," *Medical physics*, vol. 31, p. 2636, 2004.